International Journal of Concrete Structures and Materials

RESEARCH Open Access

Laboratory Investigation on Preplaced Ballast Aggregate Concrete Deterioration over Freezing–Thawing Cycles

Morteza Esmaeili[1*], Sajad Behnajad[1] and Milad Hossein Esfahani[1]

Abstract

One of the major gaps in previous research on the mechanical behavior of ballasted railway tracks converted into slab tracks using the preplaced aggregate concrete technique is its durability against freezing and thawing cycles. The present study pioneers at investigating the Preplaced Ballast Aggregate Concrete (PBAC) deterioration during freezing–thawing cycles, in which several freeze–thaw tests were carried out to measure the weight loss of PBAC samples during various freezing–thawing cycles, as well as the reduction in both compressive/tensile strengths and the relative dynamic modulus of elasticity. Moreover, the image acquisition of the PBAC samples was performed using a digital microscope and subsequently, an image processing technique was utilized to find a relation between the surface defect area at each imposed cycle and the number of cycles as a lifetime representative. As a result, an equation was developed to predict the defect frequency versus imposed cycles and the defect area generated to find the serviceability lifetime of PBAC in aggressive weather conditions. It was concluded that such PBAC can tolerate 6.16 years in the regions with full freezing–thawing weather conditions.

Keywords Preplaced ballast aggregate concrete, Freezing–thawing cycles, Compressive and tensile strengths, Regression equation, Statistical survey

1 Introduction

Preplaced Aggregate Concrete (PAC), also known as two-stage concrete and prepacked concrete, is a kind of concrete constructed by first filling a mold with coarse aggregates and then injecting sand-cement mortar into the aggregates to remove any trapped air. This method of concreting was limitedly used for the construction or repair of some dams, buildings, and bridges in the world, all by preplacing coarse aggregates into a mold (ACI, 1997). The idea of extending this method to railway track engineering was inspired by the essence of track geometry, in which the ballast layer can play the function of coarse aggregates. In order to in-situ transform ballasted tracks into slab tracks, Japanese researchers were the first to apply PAC (Railway Technical Research Institute, 1975; Odaka, 2003), followed by its applications in some sections of the South Korean metro system (Fuchigami, 2012).

In a laboratory environment, several activities have been carried out on the basis of assessing the freezing–thawing cycles on different concrete specimens. In this regard, Lee et al. investigated the effect of ballast cleanness and the quantity of redispersible polymer on the mechanical and durability properties of recycled ballast aggregate concrete through compression and flexural tests, shrinkage tests, freezing–thawing resistance tests, and optical microscopy. They have found out that a higher polymer ratio generally increases freezing–thawing resistance, modulus of rupture, and shrinkage

Journal information: ISSN 1976-0485 / eISSN 2234-1315

*Correspondence:
Morteza Esmaeili
M_esmaeili@iust.ac.ir
[1] School of Railway Engineering, Iran University of Science and Technology, Tehran 16846-13114, Iran

resistance. The freezing–thawing resistance stays almost constant for 2 to 6% of polymer usage, while it significantly increases in specimens with 10% of polymer. It was also discovered that higher mechanical and durability attributes can be achieved by higher cleanness levels of ballast aggregates (Lee, et al., 2018). Similar to the present study, Lu et al. investigated the effects of silica fume, water to binder (w/b) ratio, and fiber steel on the freezing–thawing behavior of specimens of High Performance Concrete (HPC). They have inferred that adding silica fume and reducing the w/b ratio can minimize the adverse effects of freezing–thawing cycles on concrete deterioration (Lu et al., 2021). In another study, Ebrahimi et al. conducted a multi-aspect assessment of parameters on concrete mechanism perspective under freezing–thawing cycles. Consequently, they have also revealed that nano-scaled pozzolanic additives like silica fume can sharply decrease the destructive effect of freezing–thawing cycles by filling the porosities created during construction (Baert et al., 2008; Ebrahimi et al., 2018; Panjehpour et al., 2011; Perraton et al., 1988; Zhenshuang, 2011). From a microstructural point of view, Sahin et al. attempt to describe an engineering solution for concrete structures subjected to freezing–thawing cycles. After completing additional cycles, they show that each concrete component has a unique failure regime (Şahin et al., 2021). In another survey, Ashwini et al. inferred that using silica fume can limit both relative dynamic modulus of elasticity minimization and concrete weight loss, while the increase of freezing–thawing cycles would accelerate them (Ashwini & Rao, 2021). In general, it has been repeatedly demonstrated that air-entrained concrete specimens can well withstand freezing–thawing cycles. In other words, they tolerate such aggressive weather conditions with a limited decrease in compressive strength and weight loss outputs (Neville & Brooks, 1987; Shang et al., 2014).

The background of investigating the behavior is referred to Surveys conducted by Hossein Esfahani et al. (Hossein Esfahani et al., 2021) to find the optimal injectable mortar mixture design for use in ballasted railway tracks and Esmaeili and Amiri (Esmaeili & Amiri, 2022) to assess and monitor the bending behavior of large-scale beam samples constructed by this method of concreting in railway track conditions provide the background for researching the behavior of preplaced aggregate concrete in ballasted environments. In continuation of previous researches, in order to find the application of Preplaced Ballast Aggregate Concrete (PBAC) in converting a ballasted track into a slab track system, one of the main gaps related to this subject is PBAC's resistance against freeze and thaw cycles. The significance of this topic stems from the aggressive environmental conditions that exist in Iranian railway networks. In other words, the durability of PBAC slabs is regarded as one of the Iranian railway network's hotspots because some of its locations are subjected to vast variations in weather conditions or aggressive climates. For instance, the majority of Iran's railway track networks are located in desert areas where some zones experience temperatures below − 18 °C. Since there is no evident document investigating the behavior of PBAC under freezing–thawing cycles, the present research will focus more on examining the influence of freezing–thawing cycles on the behavior of PBAC to guarantee that ballasted tracks can be converted into slab tracks under these circumstances. In this matter, firstly, several freeze–thaw tests were carried out according to ASTM C666 (ASTM C666, 2017) in order to measure the weight loss of PBAC samples during 0, 100, 200, and 300 cycles, and subsequently, the reduction in compressive and tensile strengths of PBAC specimens were assessed under the mentioned cycles. The PBAC's relative dynamic modulus of elasticity was then evaluated using the NDT ultrasonic testing method recommended in ASTM C597 (ASTM C597, 2009). In addition, an image processing technique was utilized to find a relationship between the damage area frequency and the number of cycles, focusing on the visible surface defect of specimens. For this purpose, a comprehensive statistical survey was performed on the obtained data, and subsequently, an equation was established to predict the further behavior of defect frequencies versus imposed cycles and generated defect areas. Eventually, in order to justify the obtained results, an interaction matrix and contour plot were used to find a meaningful relationship between the reciprocal influence of target measurements.

2 Laboratory Tests

2.1 Test Plan

For a meticulous investigation of the freezing–thawing cycles on PBAC specimens, the test plan presented in Table 1 was scheduled. It shall be noted that the freezing–thawing cycles for measuring the relative dynamic modulus of elasticity have been chosen according to ASTM C666 (ASTM C666. 2017) on three samples in each age and cycle, while in the case of compressive and tensile strengths, a limited number of cycles has been adopted because of the time-consuming procedure of the tests. Afterwards, the durability of PBAC samples was assessed using the procedure visualized in accordance with the flowchart shown in Fig. 1. For this purpose, the compressive and tensile strengths of specimens in each cycle, the relative dynamic modulus of elasticity in cycles introduced in ASTM C666 (ASTM C666. 2017), a visual survey and image processing were performed to define the behavior of PBAC under freezing–thawing

Table 1 Laboratory test plan

No	Cylindrical specimen dimensions (cm)	Investigated parameters	Exerted cycles	Number of specimens
1	10 × 20 (Fig. 2a)	Compressive strength—weight variation—appearance changes	0-100-200-300	12 (3 repetitions for each cycle)
2	10 × 20 (Fig. 2 (a))	Tensile strength—weight variation—appearance changes	0-100-200-300	12 (3 repetitions for each cycle)
3	10 × 30 (Fig. 2b)	Relative dynamic modulus—appearance changes	0-36-72-108-144-180-216-260-300	3

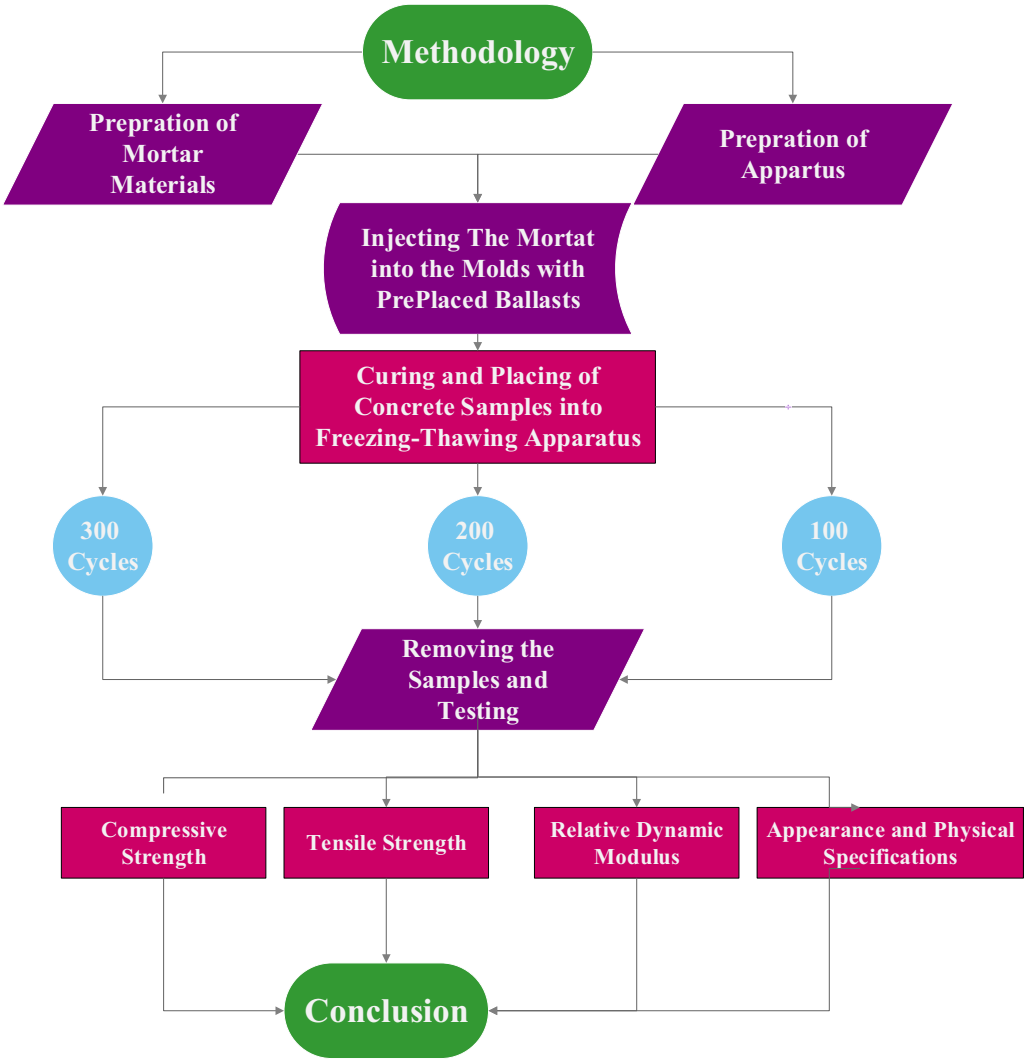

Fig. 1 Methodology and scope of the present research

conditions. The consumed materials and apparatuses are described in the following subsections.

3 Materials And Methods

In the present study, the mortars were prepared using the optimal mixture design (Table 2) of previous research (Hossein Esfahani et al., 2021) and subsequently injected into molds that have been pre-filled with ballast aggregates in order to construct PBAC specimens. The mixture design of concrete specimens, including both mortar and ballast aggregates, is given in Table 3. As is obvious from the table, the coarse aggregate and mortar volume content in each specimen are respectively calculated to be 40 and 60 percent, using an equivalent water displacement

(a) **(b)**

Fig. 2 PBAC cylindrical specimens, **a** 10 × 20 cm, **b** 10 × 30 cm

Table 2 Mixture design of mortar (Hossein Esfahani et al., 2021)

Material	Value
Cement type	Portland type I-425
Cement content (kg/m^3)	850
w/b ratio	0.35
Silica fume content (% cement)	10
Superplasticizer type	Polycarboxylate-based
Superplasticizer content (% cement)	0.36
Sand type	Silica sand of Firoozkooh
Sand combination	As Fig. 3

Table 3 Mixture design of concrete specimens

Material	Value
Coarse aggregate type	Andesite ballast
Coarse aggregate volume ratio (%)	40
Coarse aggregate density (tom/m^3)	2.26
Coarse aggregate size distribution	As Fig. 4
Mortar volume ratio (%)	60
Mortar mixture design	As Table 2

method. In this research, Portland cement type I-425, sourced from Tehran Cement Company (TCC), was used alongside silica fume with a specific surface area of 20053 m^2/kg (Hossein Esfahani et al., 2021) as cementitious materials. The mortar sand was collected from Firoozkooh's silica sand, in which the Particle Size Distribution (PSD) of each individual sand grain and the consumed combination is proposed in Fig. 3. Furthermore, the andesite ballast that acts as coarse aggregates in PBAC was prepared from the Robatkarim mine, whose PSD is illustrated in Fig. 4. In order to provide a suitable level of fluidity for mortar injection, a polycarboxylate-based superplasticizer was utilized within the recommended range of the manufacturer (Hossein Esfahani et al., 2021).

In the current research, the tests performed on concrete specimens are briefly listed in Table 4. The curing procedure has been performed using the recommendation of ASTM C192 (ASTM C192, 2016) just on the first day of sample preparation. This is due to the specimens being subjected to freezing–thawing cycles during the very early stages of concrete hardening, simulating the most critical condition of aggressive weather changes in railway tracks. On the other hand, the construction of this type of concrete in winter is considered more critical than that of summer, because concreting in winter, the fresh-state concrete encounters with both positive effect of cement hydration and adverse effect of freezing phenomenon, whereas concreting in summer only subjects the hardened concrete to frost after passing its 90-day reliable strengthening period, allowing it to better endure such conditions. Accordingly, the cylindrical

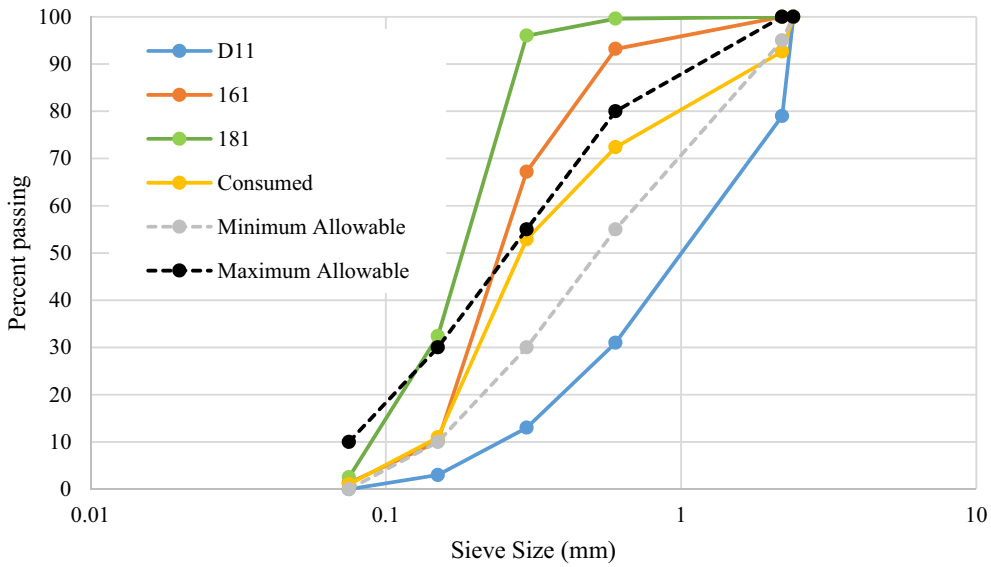

Fig. 3 Particle size distribution of Firouzkouh's sand (Hossein Esfahani et al., 2021)

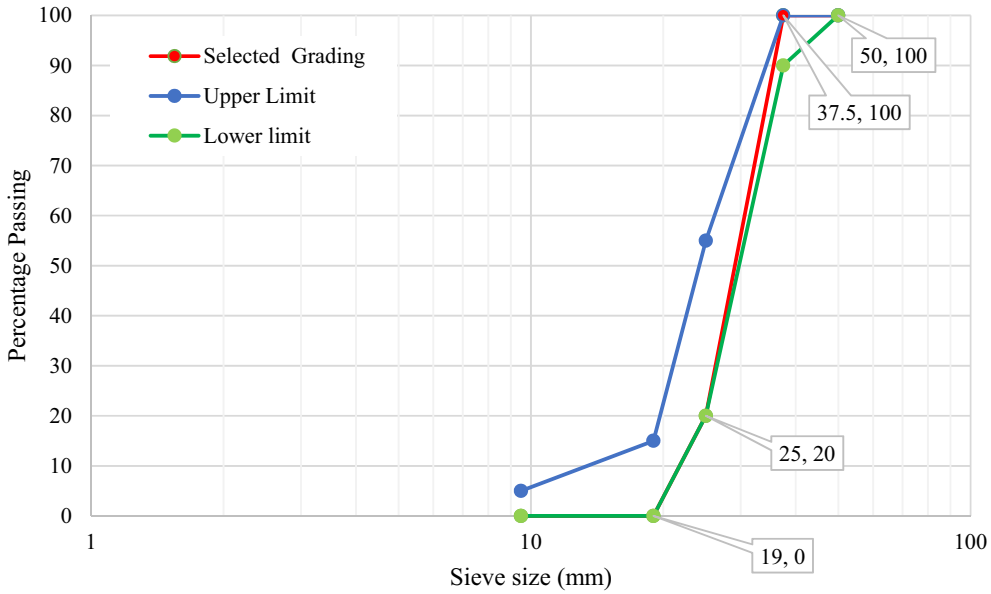

Fig. 4 Particle size distribution of Robatkarim's ballast

Table 4 Tests on concrete specimens

Test	References
Concrete compressive strength	ASTM C39, 2001
Concrete Brazilian splitting tensile strength	ASTM C496, 1986
Ultrasonic pulse velocity	ASTM C597, 2009
Image acquisition	–

specimens were first cured for one day and subsequently inserted into the chamber. After 100, 200, and 300 cycles, they were taken out just as they were starting to thaw and their compressive and tensile strengths were measured. Using the recommendations of ASTM C617 (ASTM C617, 2012), the capping procedure was performed more accurately over these specimens because the upper

surface of the cylinders would be violently damaged. It should be noted that the strength correction factor of 1.02 was multiplied to convert the rough results of 10 × 20 cm cylindrical samples into those of the standard samples (ASTM C39, 2001). One of the fundamental outputs of freezing–thawing cycles on concrete specimens is the reduction of their relative dynamic modulus of elasticity in further cycles, which is measured by ultrasonic testing recommended in ASTM C597 (ASTM C597, 2009). As depicted in Fig. 5, the velocity of the passing wave in 10*30 cm specimens was measured in each of the 36 cycles. It is notable that the acceptable value is standardized as 40% (ASTM C666. 2017).

One of the most crucial steps in a statistical approach to concrete defect detection is data gathering. In the present study, the surface scanning method was employed via a Dino Lite digital microscope, by which 146 pictures were captured from specimens with a 628 cm^2 side area. Each picture has 5,300,000 pixels. It is highlighted that the image acquisition process was performed using rotary surface scanning through five strips with a height of 4 cm, as displayed in Fig. 6. The image processing was carried out using a computer with 4 GB of graphics memory (VRAM), 12 GB of RAM, and a Core i7 CPU. This procedure was performed using Python software, the Opencv library, the visualization library of Mathplotlib, and the Jupyter Notebook programming environment. An example of an image processing procedure is given in Fig. 7. Figure (a) indicates the raw image captured by a digital microscope and after transformation into a binary form, figure (b) can be executed. The pixels in figure (b)

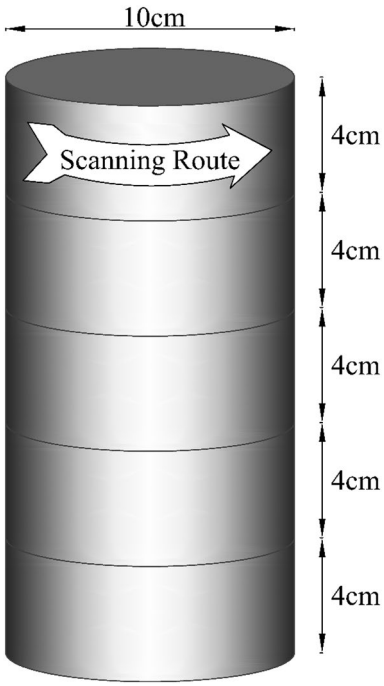

Fig. 6 Rotary image acquisition of PBAC surface

Fig. 5 Ultrasonic Pulse Velocity (UPV) test on PBAC specimens

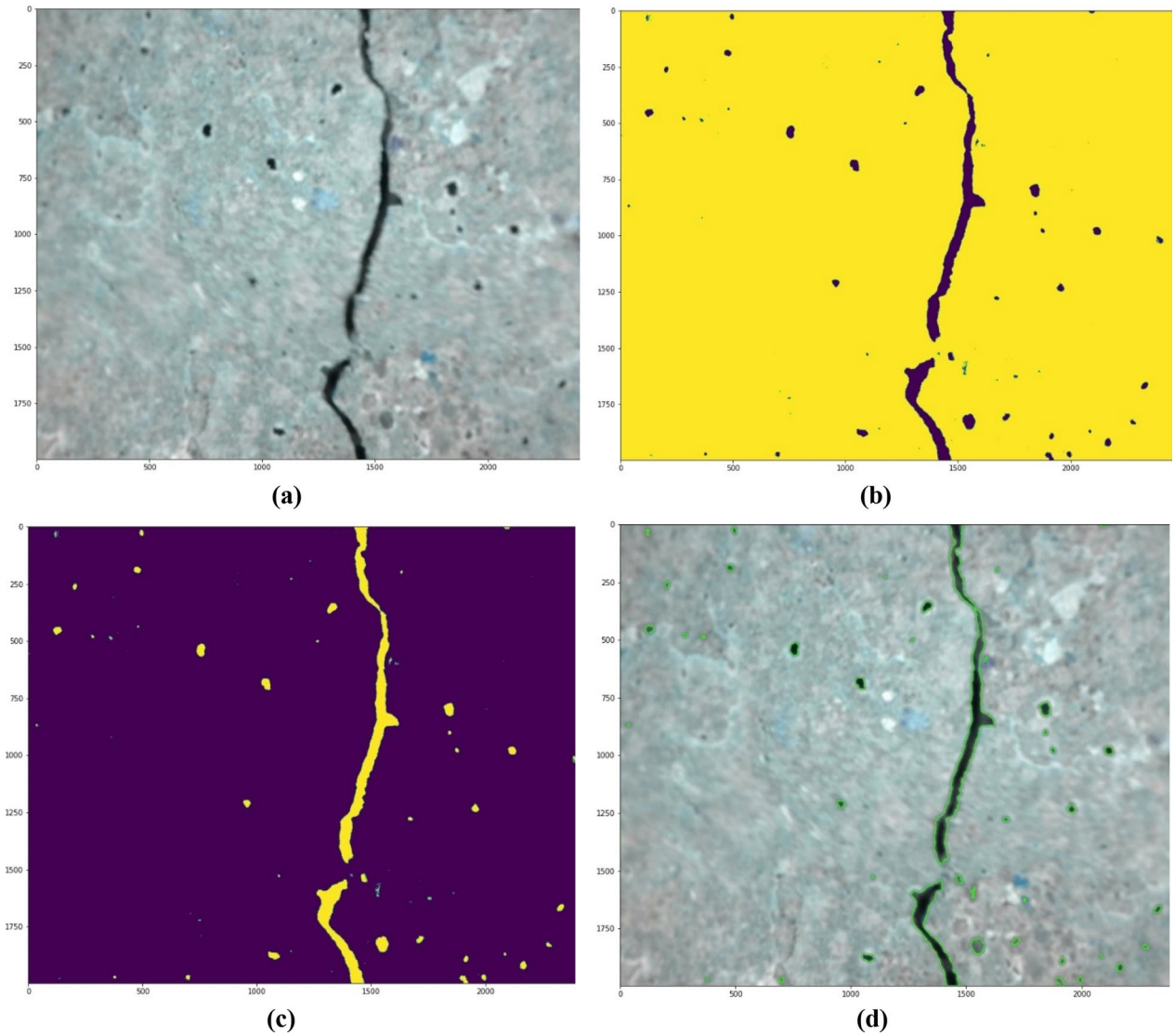

Fig. 7 Step-by-step procedure of image processing: **a** raw image, **b** image transformation into a binary form, **c** inversion of binary form, **d** defect detection in pixels

were inversed utilizing the software tools, and figure (c) was developed as a result. Following the detection of the holes, lenses, and cracks using the Opencv library and the Findcontours tool, the relevant defect area was computed in pixel units by identifying the border of each defect shown in figure (d).

3.1 Apparatuses

The prepared mortar must be homogenous and injectable through a shallow pipe. In this regard, the mixing system displayed in Fig. 8, which consists of an injection tank and an air compressor, was developed to simultaneously mix, stir, and inject the prepared mortar into the molds (ASTM C943, 2010; ASTM C938 2019). More clearly, the mortar ingredients are first added to the tank, and during mixing, constant air pressure (1.5 bars) is introduced in the pre-isolated system, causing the mortar is continuously injected into the mold. The PBAC mold, in which the ballast aggregates are preplaced, is depicted in Fig. 9. To keep the mortar from escaping, the flanges are sealed at the top and bottom of the cylindrical molds and waterproofed with polyurethane mastic. Additionally, as displayed in Fig. 10, the chamber recommended in ASTM C666 (ASTM C666. 2017) method A (developed by Azmoon Corporation) was used to investigate the freezing–thawing phenomenon on PBAC specimens. The mentioned chamber has a fridge-based apparatus in which concrete specimens are constantly subjected

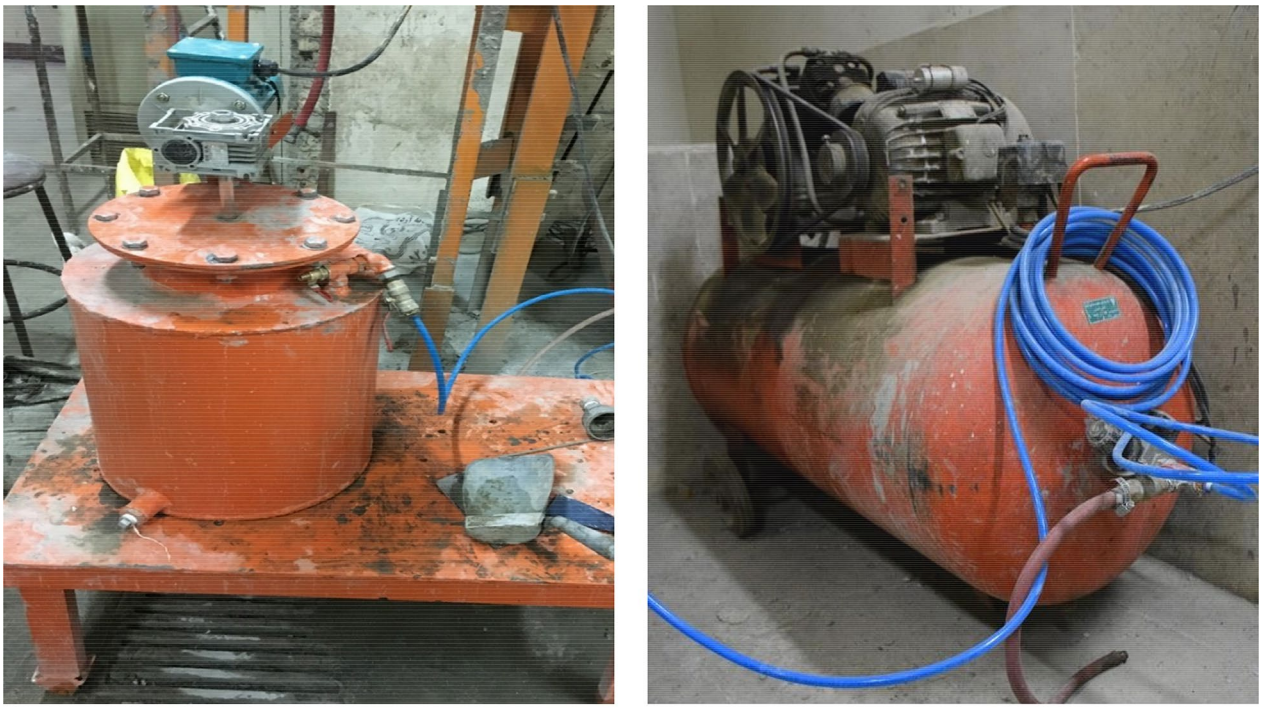

(a) **(b)**

Fig. 8 Mixing system: **a** injection tank, **b** air compressor (ASTM C938 2019)

to both freezing and thawing conditions in the − 18 to + 4 °C temperature range. For applying the mentioned temperature loading cycle, the chamber is programmed to complete each freezing and thawing procedure in three and one hours, respectively.

4 Results and Discussion

4.1 Compressive And Tensile Strength

As presented in Figs. 11 and 12, it is concluded that, despite the silica fume being consumed and the w/b ratio being low, the freezing–thawing cycles decreased the increasing trend of strength. In other words, it was expected that the specimens would gain their 28-day strength in the 100th cycle; the strength increase is clearly limited, while it is already known that the strength of silica-fume-added specimens with low ratios of w/b will dramatically increase until 90 days (Neville & Brooks, 1987). The reason for data scattering is because of the way PBAC is constructed, with the aggregates pre-filling the molds, and because the failure routes go through different shapes of aggregates or mortar (Hossein Esfahani et al., 2021). In another aspect, it is obvious that both compressive and tensile strengths of PBAC specimens stay almost constant over the cycles, which is because of the simultaneous effects of the cement and silica fume hydration on strength increase and the freezing–thawing phenomenon on strength decrease. In other words, since the specimens were exposed to freezing–thawing cycles from their very first age of construction, the hydration of cementitious materials has strengthened them, while the aggressive temperature change had a negative effect on the increase of strength. With this mechanism, the positive and negative effects would balance each other, so the strength would stay almost constant over time. It is noticeable that the mentioned scattering becomes more obvious in the 200th cycle because further observations proved that in this cycle, the generated defects appear in the form of increasing their related area. This will result in gathering various strengths in a constant mixture design and subjected cycles. From the tensile strength point of view, the strength trend is almost similar, which indicates that the reinforcement utilization in the tensile part of the PBAC slab section seems to be essential for the application of this method in railway tracks with aggressive weather conditions.

4.2 Relative Dynamic Modulus Of Elasticity

Figure 13 demonstrates three specimens with similar mixture designs subjected to up to 300 cycles. From this figure, it is well defined that the maximum decline in the relative dynamic modulus is about 11%, which represents the positive role of silica fume in

Fig. 9 PAC mold with preplaced ballast aggregates and their injection valve (ASTM C943, 2010)

strengthening specimens. Investigations performed by Lee et al. (Fig. 14) also reveal that the use of 10% silica fume significantly prevents the reduction of relative dynamic modulus (H-10), while the reduction rate of this value is more sharp in silica fume-excluded specimens (H-0) (Lee, et al., 2018). It is also clarified that using silica fume can restrict the reduction of the relative dynamic modulus of elasticity (Ashwini & Rao, 2021). By surveying the data, Eq. 1 is presented to predict the relative dynamic modulus of elasticity in cycles lower than $N_c = 900$:

$$P_C = -1.708 \ln(N_C) + 100.62 \quad , \quad R^2 = 0.947 \tag{1}$$

where P_c is the decrease in relative dynamic modulus (%) and N_c represents the number of cycles.

4.3 Weight Loss

The weight variation of concrete specimens after freezing–thawing cycles has been broadly proven to be because of generated cracking, damage to the mortar texture, segmental detachment, and loss of interstitial water in specimens with a high w/c ratio (Neville & Brooks, 1987). In the present survey, using a scale with an accuracy of 0.01 g, the average weight loss of specimens after 100, 200, and 300 cycles was recorded as 0.2151, 0.5106, and 0.9107 percent, respectively. Results of Fig. 15 indicate that the maximum value of weight loss in 300 cycles is below 1%, which highlights the acceptable resistance of PBAC specimens from this standpoint. It is worth noting that similar results have been obtained in railway

(a) **(b)**

Fig. 10 Freezing and thawing apparatus:, **a** chamber **b** frozen specimens (ASTM C666 2017)

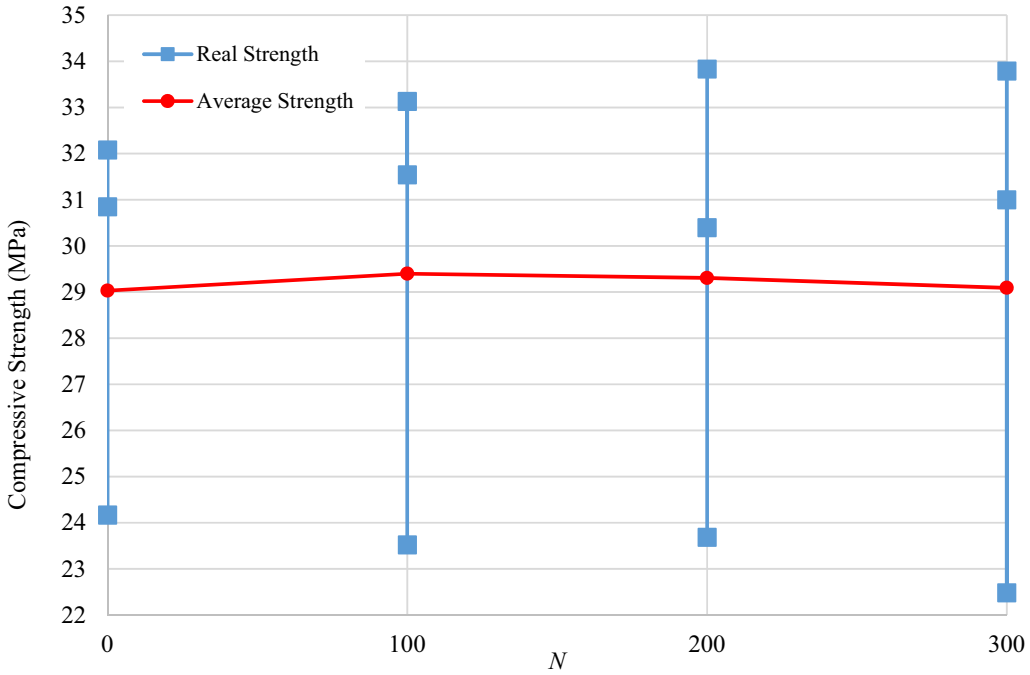

Fig. 11 Compressive strength of specimens

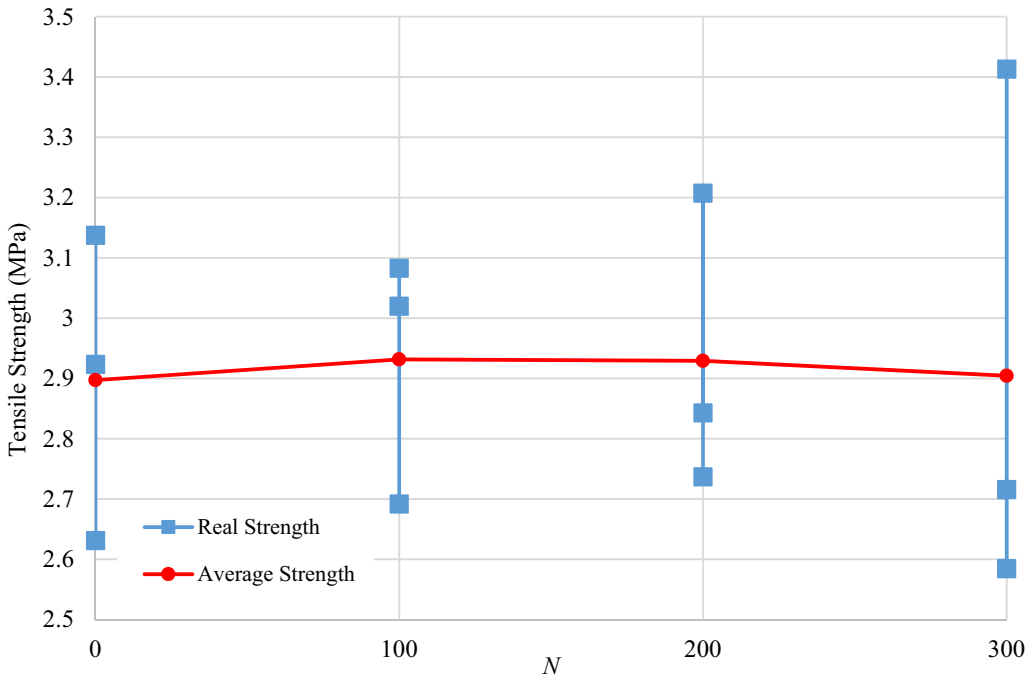

Fig. 12 Tensile strength of specimens

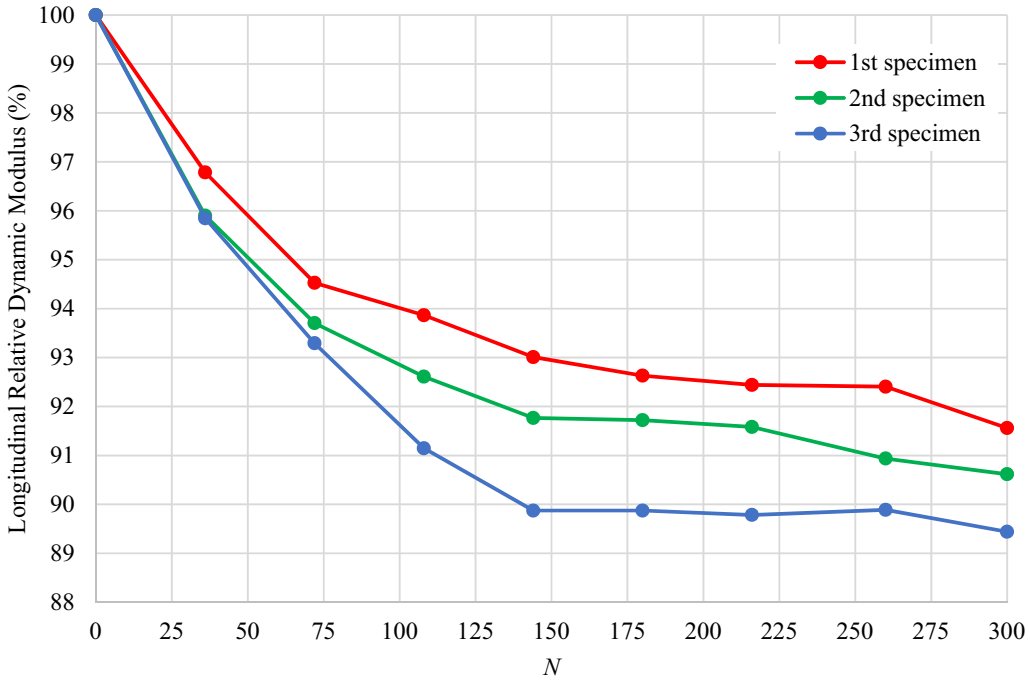

Fig. 13 Reduction percentage of relative dynamic modulus over cycles

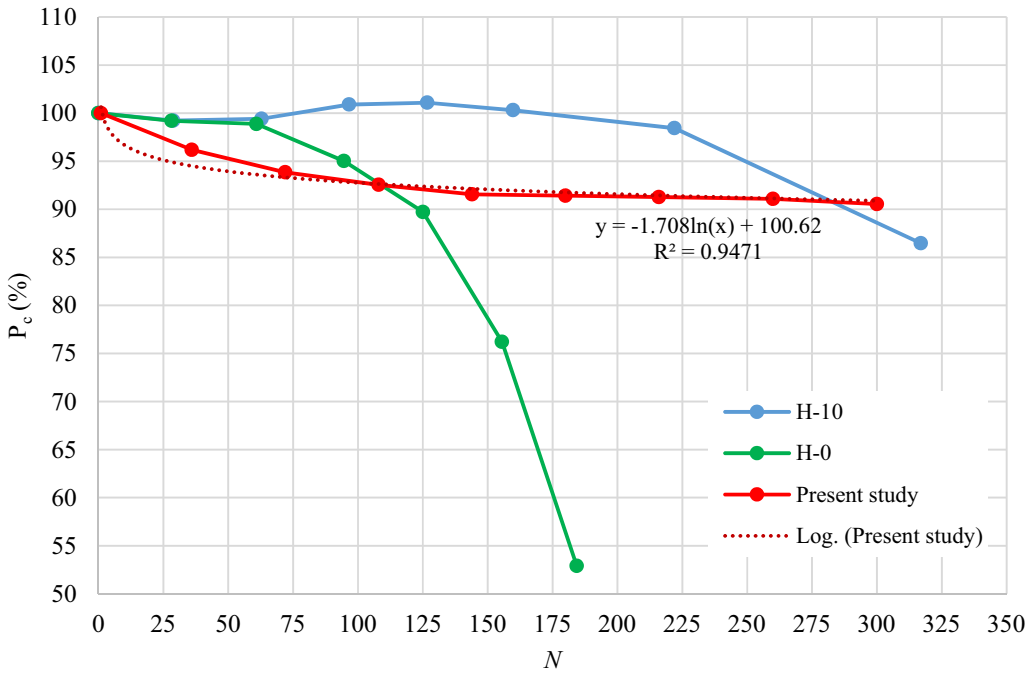

Fig. 14 Comparison of relative dynamic modules

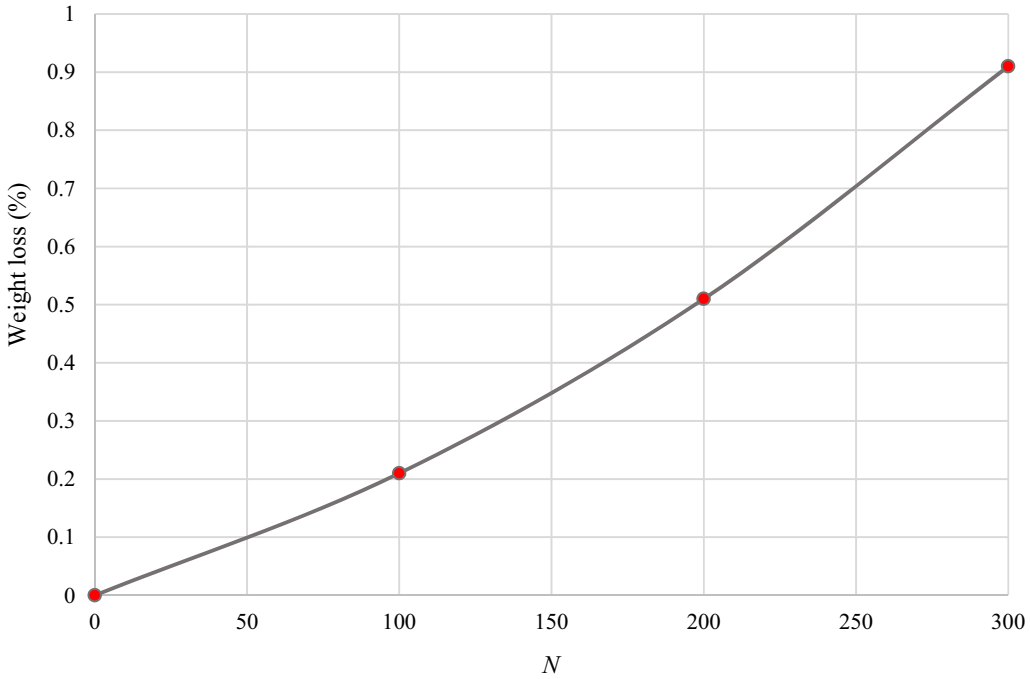

Fig. 15 Weight loss of PBAC specimens versus freezing–thawing cycles

Fig. 16 Dino Lite digital microscope

concrete sleepers as a representative of HPC concrete (Albahttiti et al., 2013).

4.4 Image Acquisition And Analysis

To inquire about the appearance changes in PBAC specimens after 100, 200, and 300 cycles, a Dino Lite digital microscope was adopted in addition to an unarmed eye inspection for crack detection and defect recognition. The image acquisition was performed with a unit length accuracy of 200 μm using the apparatus displayed in Fig. 16.

There was no apparent defect detected before 100 cycles. However, the 100th cycle commenced with an initial flaw on the specimen surface in the form of mini-lens and mini-hole shapes. As presented in Fig. 17a–c, a wide area of the specimen surface stays flawless, yet some mini-holes are generated. The surface scanning presented in Fig. 17d indicates that the defects are just ice lenses in the mortar and lens-hole combinations in the concrete Interfacial Transition Zone (ITZ). In the 200th cycle, the growth of defects results in an increase in the number of holes and lens. As indicated in Fig. 18a, the surface of specimens with a freezing–thawing experience of 200 cycles is reshaped into a dotted and rough form, and in Fig. 18b–d, it is well clarified that the number of defects has increased in both the ITZ area and cement matrix texture. In the 300th cycle, the defect development rate has sharply increased so that the holes were unified, surface cracks were generated, and the major holes were clearly apparent with an unarmed eye (Fig. 19a, b). It is understandable from Fig. 19c that in further cycles, the holes and lenses are transformed into cracks in PBAC's weak areas like ITZ. Also, the mortar texture investigations in Fig. 19d–f show more critical surface defects in the 300th cycle from their width and depth standpoints.

Overall, it can be inferred that the strength decrease in further cycles can be justified by the fact that the failure path tends to pass across the ITZ area and specimen core in compression tests, while in initial cycles, the failure was generally seen in the specimen surface. This can clearly address the progressive damage

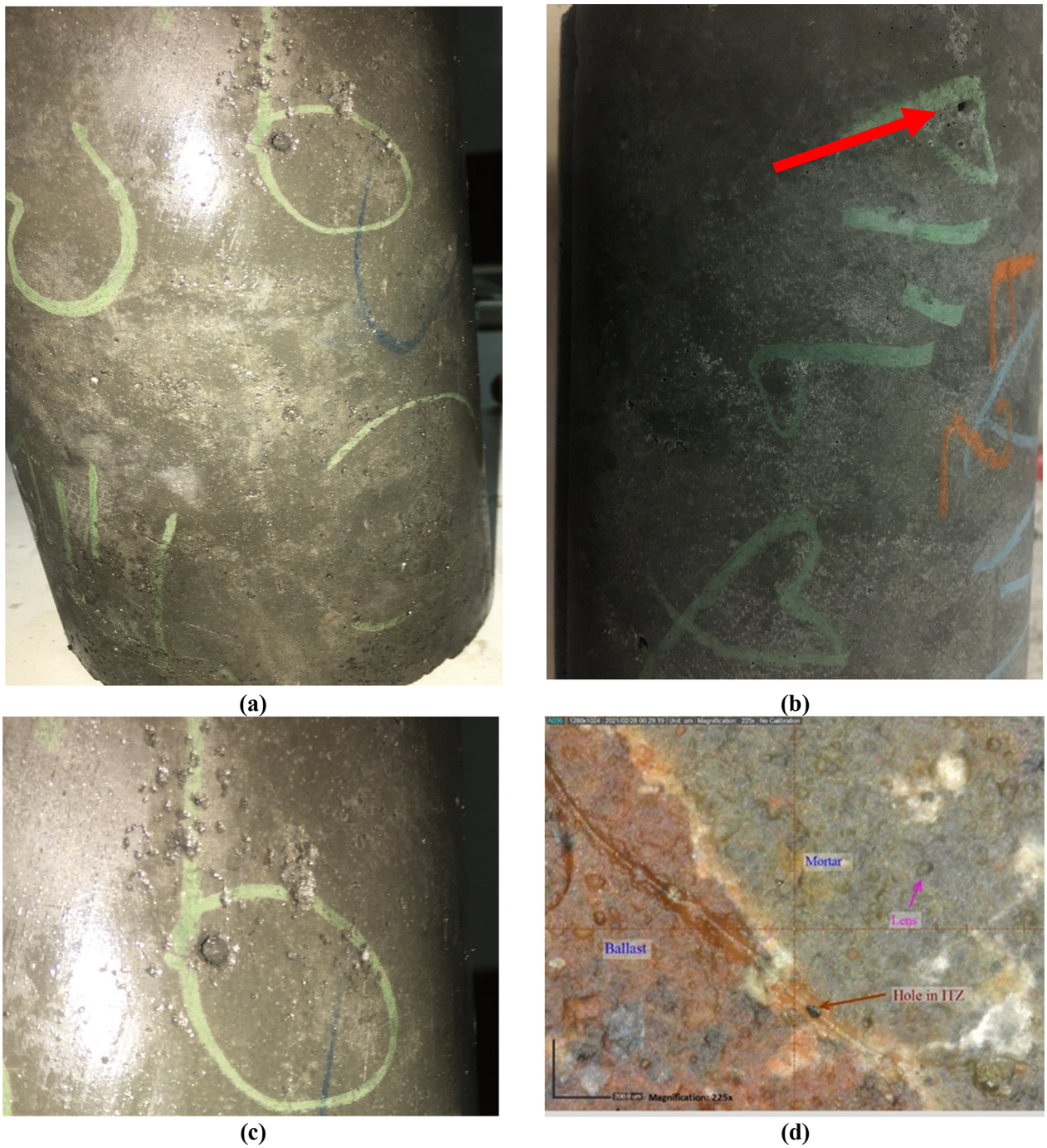

Fig. 17 Surface of PBAC specimens after 100 cycles: **a**–**c** visual inspection, **d** digital image from ITZ (225X)

to specimens through their depth in higher cycles. In addition, as is obvious from the figures, the number and area of defects have increased in further cycles. This is because of the gradual deterioration of specimens under both frequent freezing–thawing cycles and water volumetric expansion into the concrete texture. In other words, as the number of freezing–thawing cycles increases, defects like holes and lenses start to spread through the surface and depth. This will continue until more strong zones of concrete are also affected, and eventually the entire structure of the specimen is weakened. It is notable that the existence

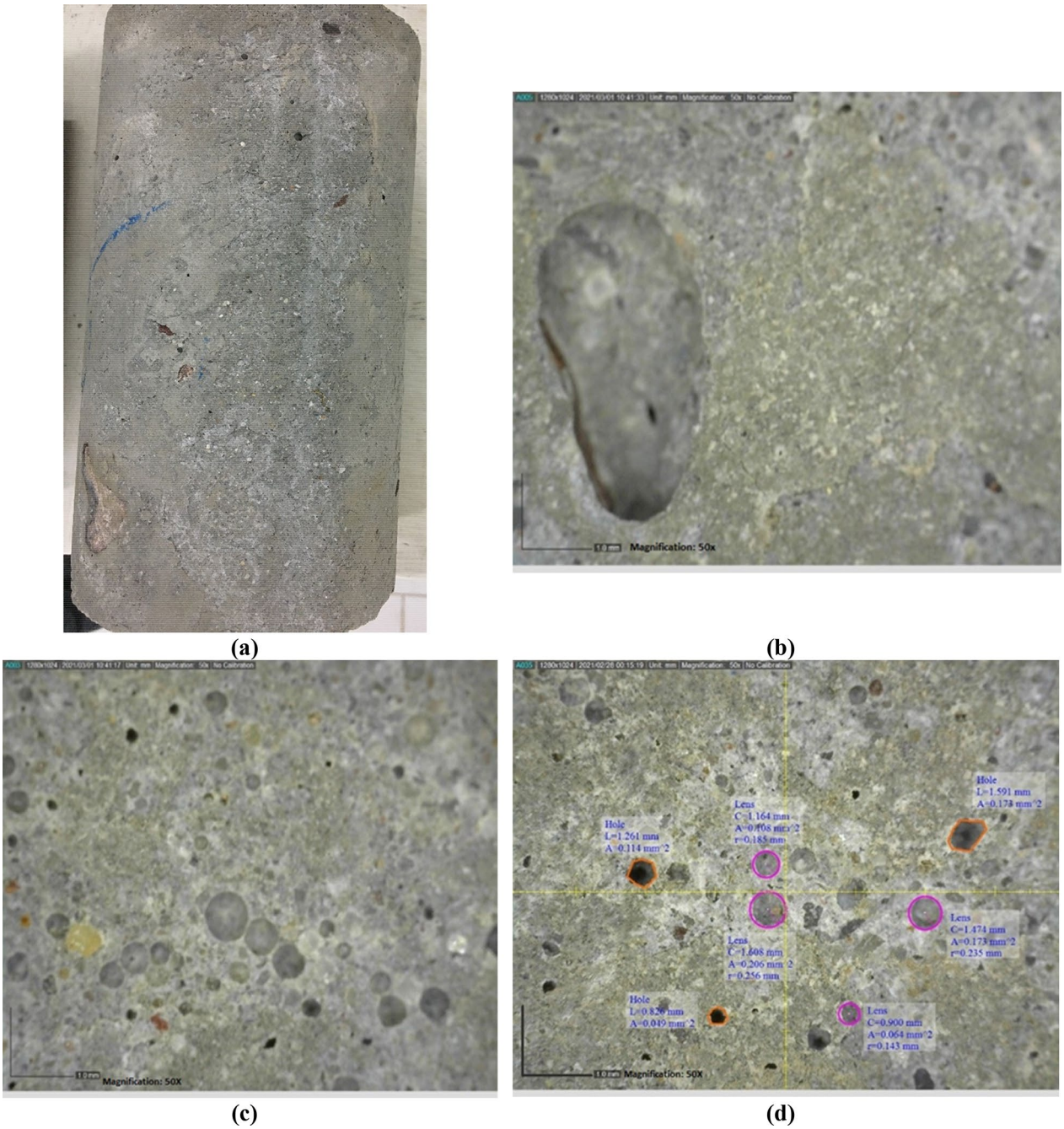

Fig. 18 Surface of PBAC specimens after 200 cycles: **a** visual inspection, **b**–**d** digital images from mortar (50x)

of silica fume as a micro-scaled additive plays a key role in preventing more serious damages in comparison with those of silica fume-excluded specimens because of its porosity-filling characteristics (Ebrahimi et al., 2018; Lee, et al., 2018; Lu et al., 2021). A comprehensive schema of defect growth over passing cycles is illustrated in Fig. 20.

4.5 Statistical Analysis Of The Results

4.5.1 Statistical Survey

As a primary conclusion, it seems important to draw the results of image processing. Fig. 21a demonstrates the raw outputs of image processing, but due to the illegibility of recorded data and their related trends, Fig. 21b was developed as a modified version by imposing correction filters using the mean

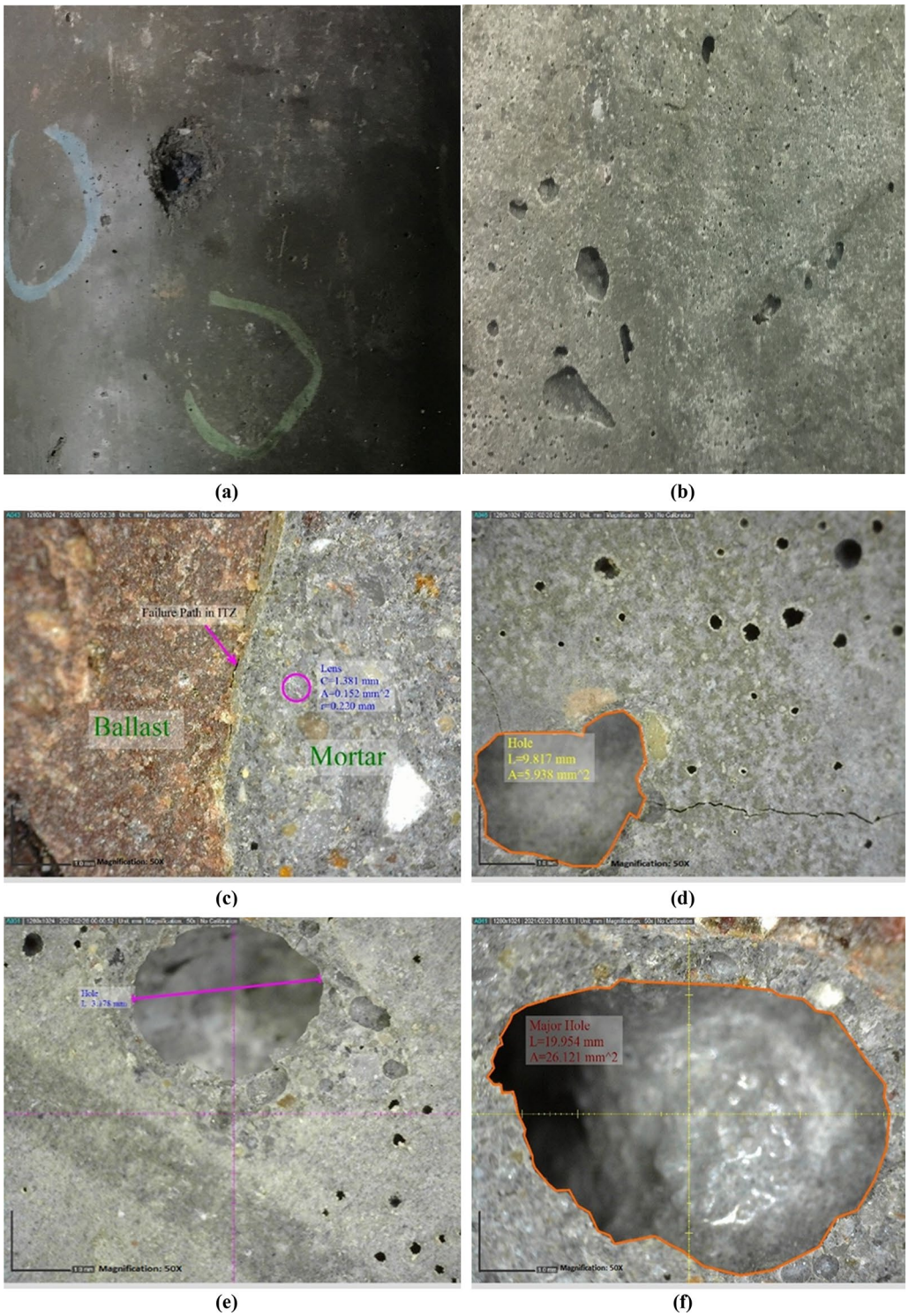

Fig. 19 Surface of PBAC specimens after 300 cycles: **a**, **b** visual inspection, **c** digital image from ITZ (50x), **d**–**f** digital images from mortar (50x)

interpolation method. As a result, it can be concluded from Fig. 21 that 200th cycle has made the defects of previous cycles more frequent from a countdown standpoint, while in the 300th cycle, the recorded area was reduced and the sum of all logged defect areas was increased, which means that the majority of

Fig. 20 Schema of surface defect growth over passing cycles

defects have sharply increased and some cracks have been generated due to the unification of the individual defects in both the cement paste matrix and the ITZ zone.

Assessing the data of surface scanning by Minitab statistics software has revealed that the area of generated defects in each cycle follows the statistical Gamma distribution with the density histogram and calculated parameters presented in Fig. 22 and Table 5. The higher values of variance and beta in the 200th cycle also justify that there is a meaningful difference in area increase in this cycle.

4.5.2 Regression Equations

Using the incorporation of MATLAB and Minitab software, a multi-parameter regression was developed based on the obtained laboratory data to evaluate the behavior of PBAC specimens under freezing–thawing cycles and to forecast their strength in further cycles. In this regard, Eq. 2 is proposed to predict the strength variation of this kind of concrete in various cycles:

$$f_{cn} = aN^3 + bN^2 + cN + d,\ R^2 = 1 \tag{2}$$

where f_{cn} is the normalized compressive or tensile strength of specimens expressed as a strength ratio, N is the number of freezing–thawing cycles exerted, and a to d are constants whose values are listed in Table 6.

Fig. 23 illustrates the compressive or tensile strength ratios. Clearly, the strength increase in the 100th cycle is due to the advantage of cement hydration upon destructive freezing–thawing cycles, but in further cycles, it can be clarified that the cement hydration is almost stopped (after 28 days of PBAC age) and the effect of freezing–thawing cycles seems to be more dominant in strength reduction. For extensive research, the two-parameter formula of Eq. 3 was used with nonlinear regression algorithms to predict the behavior of PBAC after certain cycles, which is not supported by economic logic or standard recommendations. Moreover, the real values versus their predicted values (Eq. 3) are proposed in Fig. 24. From this figure, it can be seen that the prediction seems to be more accurate in prior cycles.

$$F = 1.46Ne^{-0.00887A} + 5.54,\ R^2 = 0.8 \tag{3}$$

where F is the frequency of generated defects under N freezing–thawing cycles and A represents the defect area in pixels.

4.5.3 Output Interactions

In the present study, an interaction matrix plot and contour were developed to assess the mutual influence of each parameter on the desired parameters. For this purpose, it can be concluded from Fig. 25 that there is no predictable strength behavior of PBAC specimens over passing cycles, just because of its simultaneity with cement hydration and the early freezing phenomenon, but it is evident that the relative dynamic modulus of elasticity reduction and the weight loss rate will be enhanced in further cycles. As is well known in the classic strength of materials literature, higher values of dynamic modulus generally represent higher strength of concrete specimens. Fig. 26 implies that there is no serious difference

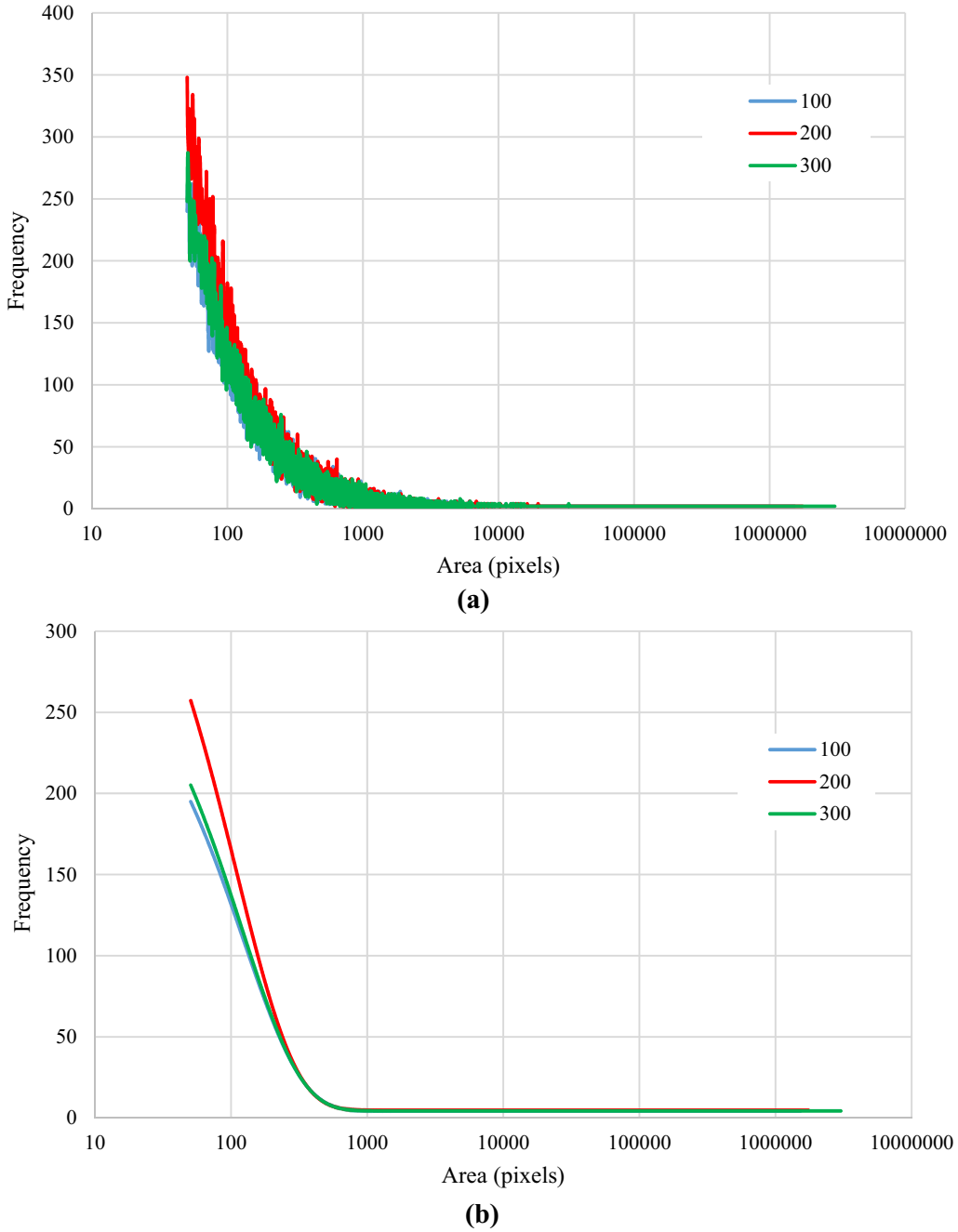

Fig. 21 Results of image processing: **a** raw outputs, **b** modified outputs

in the reduction of both relative dynamic modulus and compressive strength in cycles lower than 100. Therefore, it can be deduced that PBAC specimens can withstand the aggressive weather conditions for approximately 100 cycles, whereas the deterioration of intact structure will begin in further cycles, depending on the mixture design.

4.5.4 PBAC Lifetime Prediction

The prediction of PBAC's lifetime under freezing–thawing conditions shall be highlighted for recognition of the final serviceability of the constructed slab track. For this purpose, Fig. 27 was developed using the prediction reduction equation proposed in previous sections. Since

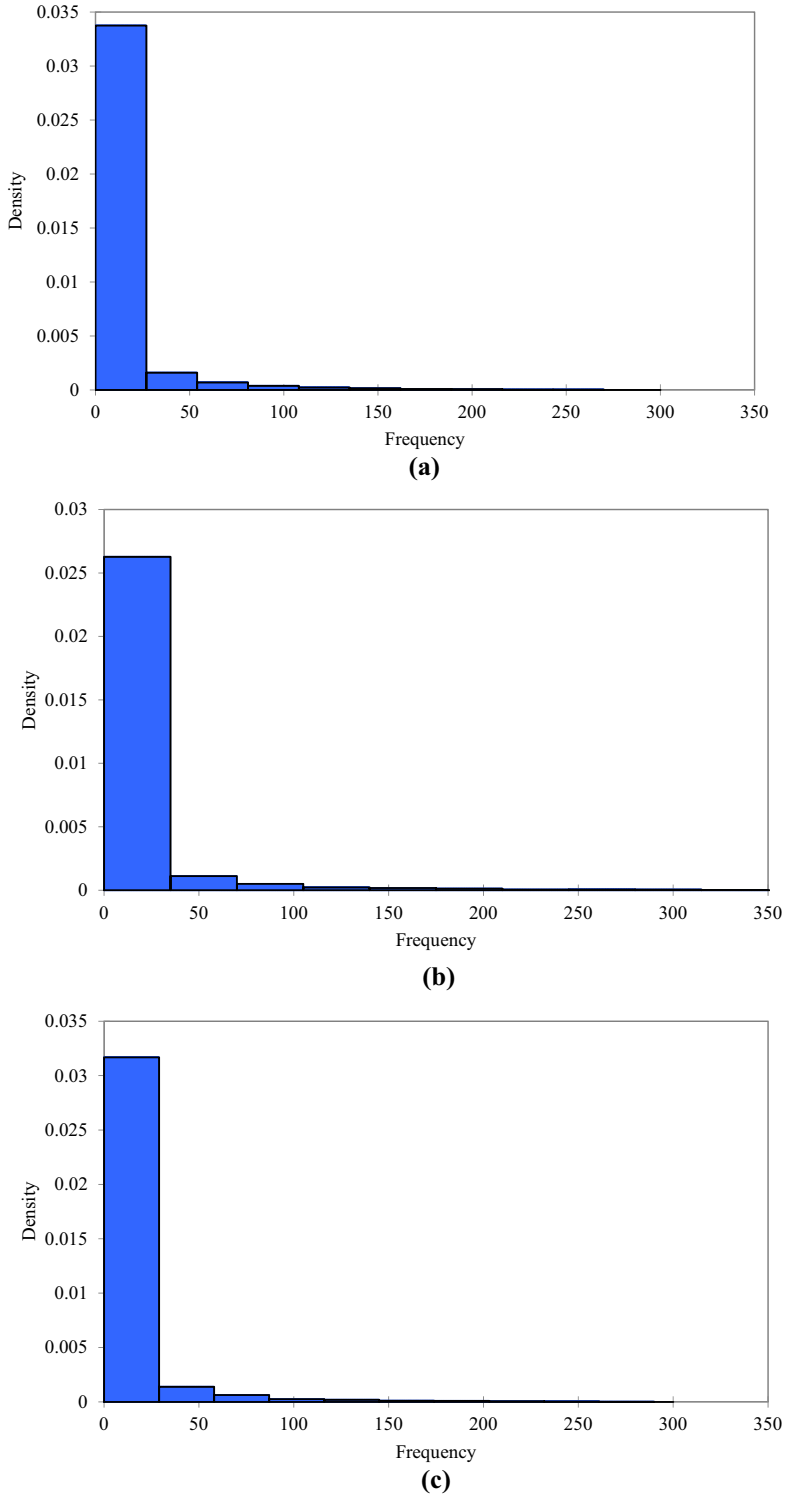

Fig. 22 Gamma density histograms for each cycle: **a** N = 100, **b** N = 200, **c** N = 300

the maximum allowable reduction percentage of relative dynamic modulus is introduced as 40% (ASTM C666. 2017), supposing this value for both compressive and tensile strength reduction, the corresponding number of cycles was evaluated using the extracted linear regression equations in the 100th cycle onwards in Fig. 23. This value is also considered the final lifetime serviceability of the PBAC slab. Thoroughly, Fig. 27 declares that the service

Table 5 Statistical parameters of Gamma distribution

Cycle	Statistical parameter	Real value	Estimated value
100	Mean	10.81	10.81
	Variance	614.23	614.23
	Skewness	5.17	4.59
	k	–	0.19
	Beta	–	56.83
	D value of Kolmogorov–Smirnov test	–	0.57
200	Mean	12.61	12.61
	Variance	985.49	985.49
	Skewness	5.43	4.98
	k	–	0.16
	Beta	–	78.15
	D value of Kolmogorov–Smirnov test	–	0.59
300	Mean	10.62	10.62
	Variance	634.17	634.17
	Skewness	5.41	4.74
	k	–	0.18
	Beta	–	59.72
	D value of Kolmogorov–Smirnov test	–	0.59

Table 6 Constants of strength ratio

Normalized target	a	b	c	d
Compressive strength	2e-9	− 1e-6	0.0002	1
Tensile strength	8e-10	− 9e-7	0.0002	1

cycle number of a PBAC slab is defined as infinite from a dynamic modulus standpoint. Nevertheless, from both compressive and tensile strength points of view, it is clear that 9000 cycles are required to reach the 40% strength reduction. Since in the freezing–thawing test, each cycle lasts for six hours ($^1/_4$ day), this value is transformed into $9000 \times {}^1/_4 \times {}^1/_{365} = 6.16$ years as the final serviceability lifetime of the PBAC slab. It means that this type of slab can only last 6.16 years under permanent freezing–thawing weather conditions.

Considering there are various weather conditions in the world, it is essential to extend the results for the total serviceability of PBAC slabs in different frost-experiencing weather conditions. In this regard, it is obvious that the PBAC slab lifetime will decrease in regions that experience further months of aggressive weather conditions. Equation 4 is developed to consider the lifetime reduction of PBAC slabs in regions with different frost regimes:

$$Lifetime = \frac{6.16 \times 12\,(months)}{M} \tag{4}$$

where *lifetime* is the total serviceability of PBAC slabs (year) and M is the number of frost months experienced in the region.

Figure 28 is drawn based on Eq. 4 for regions that experience different numbers of frost months per year. Taking into account the 60-year total allowable slab lifetime suggested in IRS 70727 (Appendix D) (IRS 70727-1, 2021), the region where the PBAC slab is installed must not experience more than 1.23 months (37 days) of aggressive freezing–thawing cycles per year. It also states that the PBAC slab endures just 6.16 years in the regions that experience absolute frost for an entire months of the year.

5 Conclusions

The novelty of this research lies in the comprehensive investigation of the influence of freezing–thawing cycles on the mechanical behavior of preplaced ballast aggregate concrete (PBAC). In this regard, the following conclusions can be drawn:

- Freezing–thawing cycles cause the reduction in strength enhancement from 28 days. Investigations proved that by passing the 300th cycle, the concrete specimen strength starts to diminish. The addition of silica-fume and a low w/b ratio well prevent the negative effect of such aggressive conditions from a strength standpoint.
- An ultrasonic non-destructive test was performed on PBAC in each of the 36 cycles of freezing and thawing. After 300 cycles, an 11% reduction in the relative dynamic modulus of elasticity was recorded, which meets the standard criterion.
- In the most critical situation, the weight loss of silica-fume added PBAC specimens did not exceed 1%, which demonstrates the positive role of this additive in this domain.
- An unarmed visual inspection uncovered that the passing freezing–thawing cycles will result in changes in PBAC's surface defect shapes. In this regard, the imperfections were demonstrated in lenses and holes until the 200th cycle, joining together to generate cracks in the 300th cycle. However, there was no severe defect on the PBAC specimen surface due to the existence of silica fume as a strong binder.
- A two-parameter non-linear regression was developed to forecast the PBAC defect frequency over imposed freezing–thawing cycles and the generated

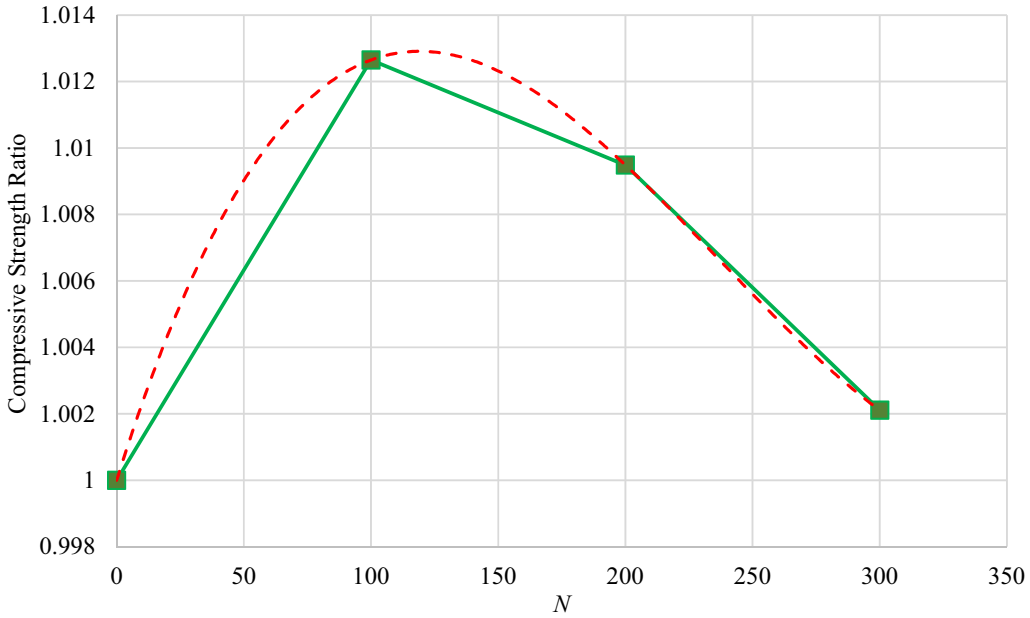

(a)

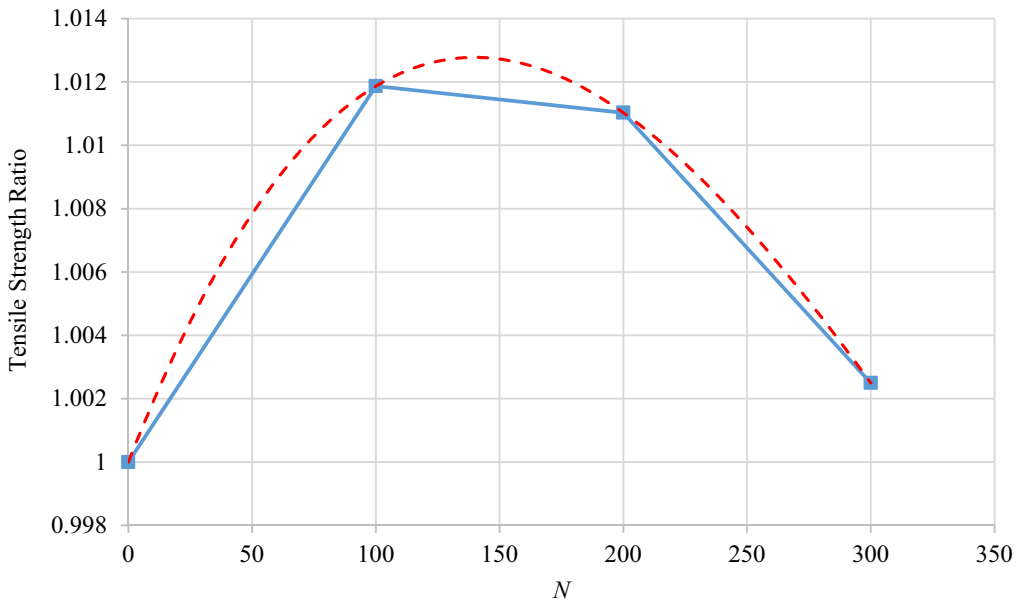

(b)

Fig. 23 Strength ratio diagrams of PBAC specimens: **a** compressive strength, **b** tensile strength

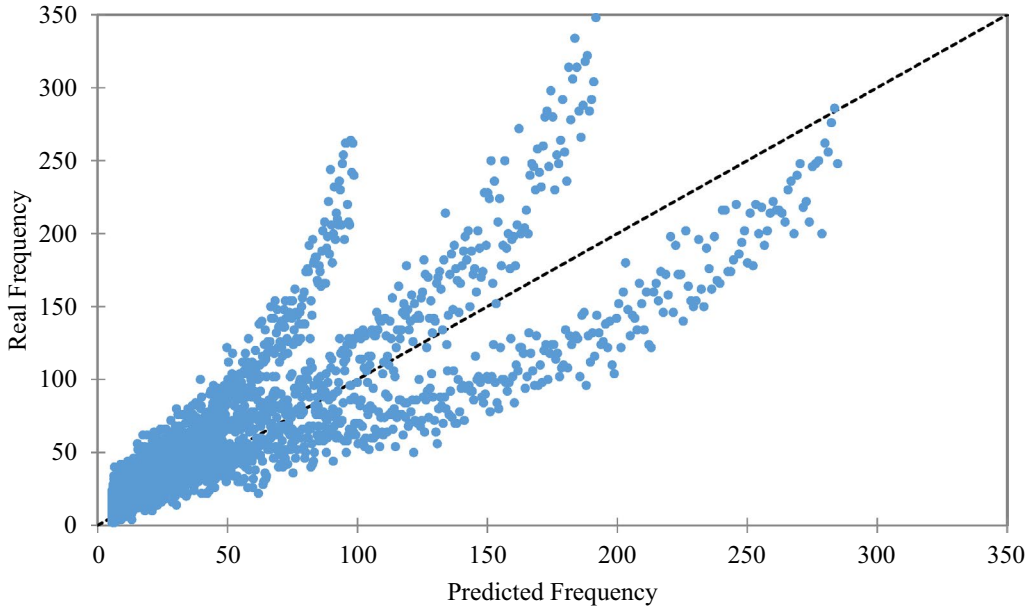

Fig. 24 Real value versus predicted values of defect frequency

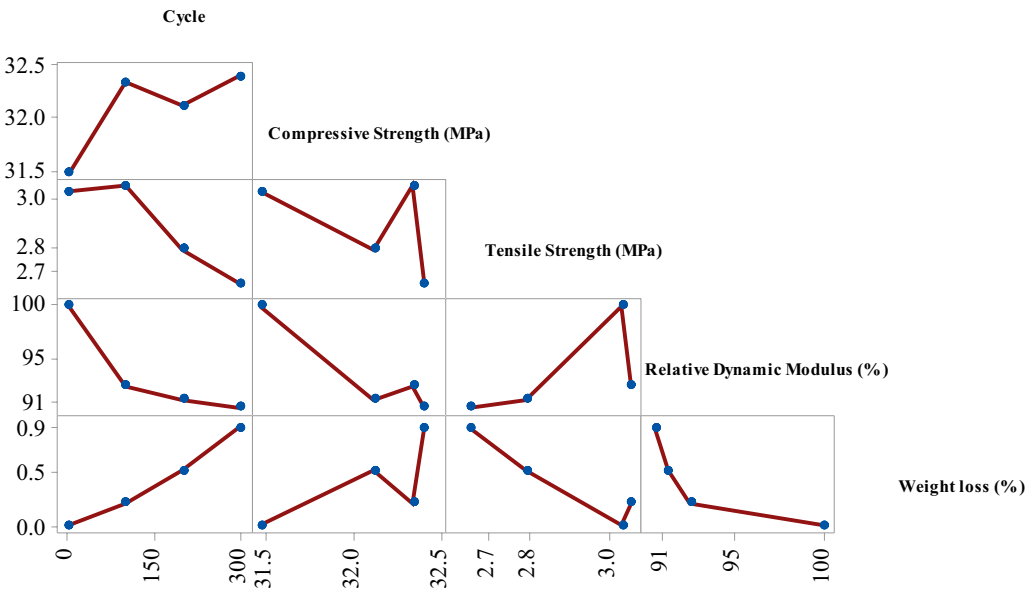

Fig. 25 Interaction matrix plot of research outputs

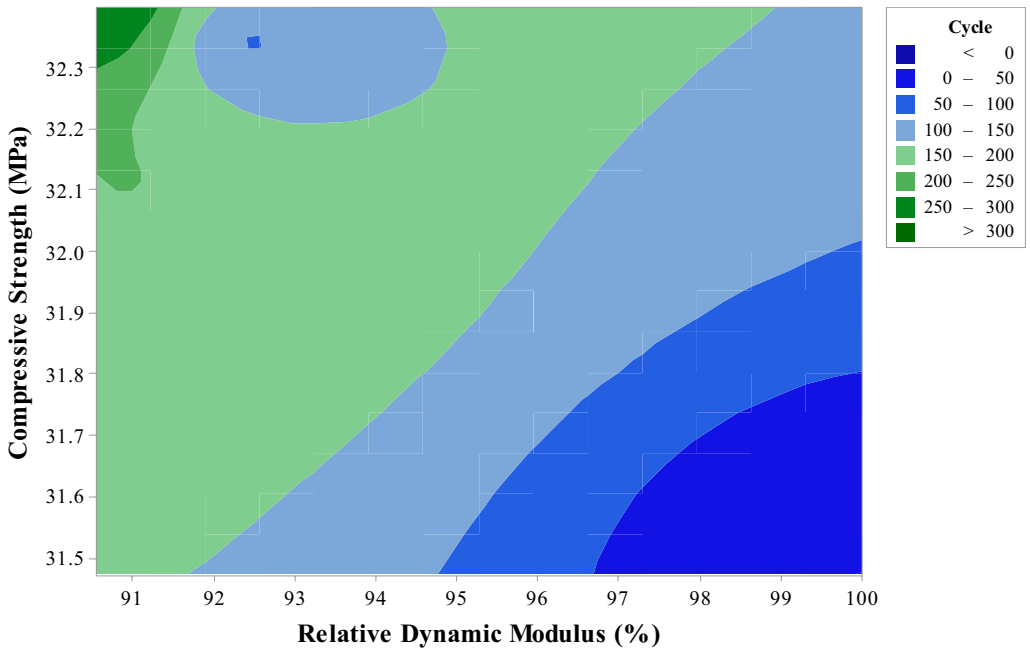

Fig. 26 Contour plot of two main results over passing cycles

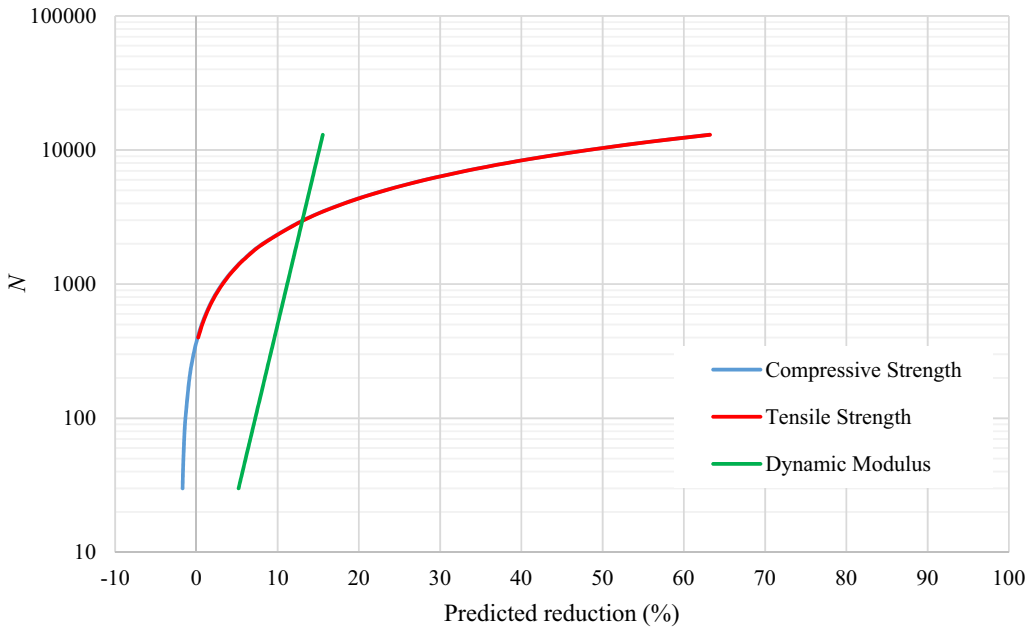

Fig. 27 Lifetime prediction diagram of PBAC slab

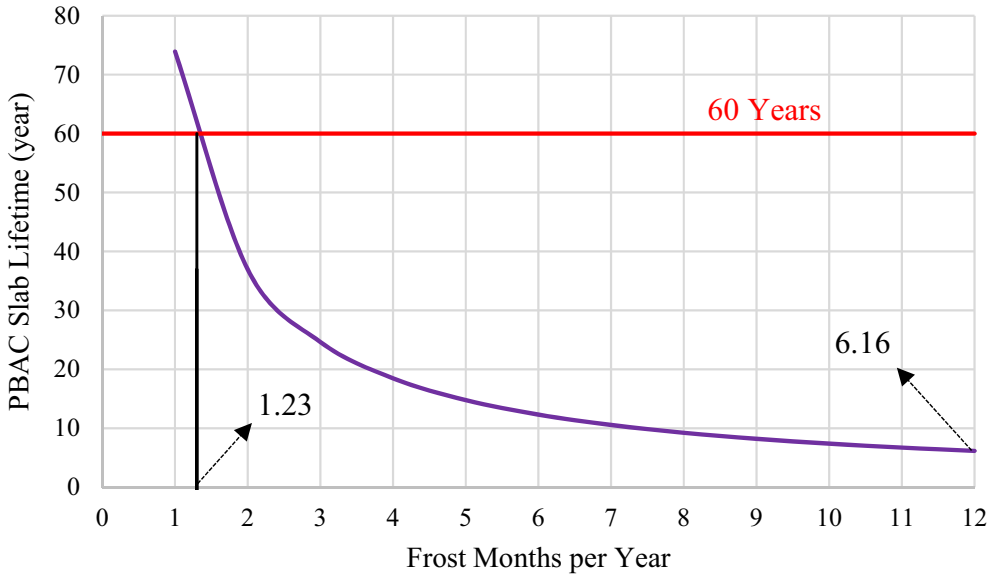

Fig. 28 PBAC service lifetime in various weather conditions

defect area. Subsequently, using statistical methods for lifetime prediction, it is discovered that a PBAC slab can withstand 6.16 years of permanent aggressive weather conditions. Moreover, only 37 days of freezing–thawing cycles per year are permitted for such a slab to remain serviceable for 60 years.

Acknowledgements
The research team acknowledges the support of the personnel of School of Railway Engineering in Iran University of Science and Technology (IUST). The authors would like to thank Eng. Mohsen Paricheh for creating the professional illustrations for this paper.

Author contributions
M.E: Supervising, test planning, results analyzing, paper writing editing. S.B: Conducting the tests, instrumentations, data gathering, writing the paper. M.H.E: Statistical analyses, results analyzing, paper writing editing. All authors read and approved the final manuscript.

Authors' information
Morteza Esmaeili received his Ph.D. degree in Geotechnical Engineering from Faculty of Engineering in Tehran University, Tehran, Iran, in 2004. Now he works at Iran University of Science and Technology, School of railway Engineering as full-time professor. His current research interests include railway dynamics, railway geotechnics and ballastless railway tracks.
Sajad Behnajad is M.Sc. graduate from Iran University of Science and Technology, School of railway Engineering. His current expertise is concrete technology focusing on freezing-thawing assessment of concrete in aggressive weather conditions.
Milad Hossein Esfahani is currently a Ph.D. candidate in railway engineering at Iran University of Science and Technology. His research career is concrete technology focusing on Preplaced Aggregate Concrete and its application in the field of railway track engineering.

Funding
The authors have not received any funding from anywhere for doing the research.

Availability of data and materials
The data that support the findings of this study are available from the corresponding author upon reasonable request.

Declarations

Ethics approval and consent to participate
Not applicable.

Consent for publication
Not applicable.

Competing interests
The authors declare that they have no competing interests.

Received: 4 November 2022 Accepted: 17 April 2023
Published online: 21 August 2023

References
ACI. (1997). *ACI 304 guide for the use of pre placed aggregate concrete for structural and mass concrete applications*. American Concrete Institute.
Albahttiti, M., Ghadban, A., Riding, K., & Stuart, C. (2013). Freeze-thaw performance testing of whole concrete railroad ties.
Ashwini, K., & Rao, P. S. (2021). Freeze and thaw resistance of concrete using alccofine and nano-silica. *Materials Today Proceedings, 47*, 4336–40.
ASTM C192. (2016). *Standard practice for making and curing concrete test specimens in the laboratory*. ASTM International.
ASTM C39. (2001). *Standard test method for compressive strength of cylindrical concrete specimens*. ASTM international West Conshohocken.
ASTM C496. (1986). *Standard test method for splitting tensile strength of cylindrical concrete specimens*. ASTM international.
ASTM C597. (2009). *Standard test method for pulse velocity through concrete*. ASTM International.

ASTM C617. (2012). *Standard practice for capping cylindrical concrete specimens*. ASTM International West Conshohocken.
ASTM C666. (2017). Standard Test Method for Resistance of Concrete to Rapid Freezing and Thawing.
ASTM C938. (2019). *Standard practice for proportioning grout mixtures for preplaced-aggregate concrete*. ASTM international West Conshohocken.
ASTM C943. (2010). *Standard Practice for Making Test Cylinders and Prisms for Determining Strength and Density of Preplaced-Aggregate Concrete in the Laboratory*. American Society for Testing and Materials.
Baert, G., Poppe, A. M., & De, B. N. (2008). Strength and durability of high-volume fly ash concrete. *Structural Concrete, 9*(2), 101–108.
Ebrahimi, K., Daiezadeh, M. J., Zakertabrizi, M., Zahmatkesh, F., & Korayem, A. H. (2018). A review of the impact of micro- and nanoparticles on freeze-thaw durability of hardened concrete: mechanism perspective. *Construction and Building Materials, 186*, 1105–1113.
Esmaeili, M., & Amiri, H. (2022). Laboratory investigation into the flexural behavior of embedded concrete sleepers in two-stage concrete with preplaced ballast aggregate. *International Journal of Concrete Structures and Materials*. https://doi.org/10.1186/s40069-021-00487-4
Hossein Esfahani, M., Esmaeili, M., & Tadayon, M. (2021). The effects of admixtures on the mechanical behavior of preplaced ballast concrete for use in slab track systems. *International Journal of Pavement Research and Technology, 2021*, 1.
IRS 70727-1ed. (2021). Railway application—track superstructure decision-making.
Lee, S., et al. (2018). Effects of redispersible polymer powder on mechanical and durability properties of preplaced aggregate concrete with recycled railway ballast. *International Journal of Concrete Structures and Materials*. https://doi.org/10.1186/s40069-018-0304-1
Lu, Z., Feng, Z.-G., Yao, D., Li, X., & Ji, H. J. C. (2021). Freeze-thaw resistance of Ultra-High performance concrete: dependence on concrete composition. *Construction and Building Materials, 293*, 123523.
Neville, A. M., & Brooks, J. J. (1987). *Concrete technology*. Longman Scientific & Technical.
Odaka, T. (2003). Development of low-maintenance railway tracks using the full-size railway track testing. *JREA, 46*, 23–25.
Panjehpour, M., Ali, A. A., & Demirboga, R. (2011). A review for characterization of silica fume and its effects on concrete properties. *International Journal of Sustainable Construction Engineering and Technology, 2*, 2.
Perraton, D., Aiticin, P. C., & Vezina, D. (1988). Permeabilities of silica fume concrete. *Special Publication, 108*, 63–84.
Railway Technical Research Institute. (1975). *Properties of quick hardening cement, asphalt grout, and concrete and their practical problems*. Railway Technical Research Report. Railway Technical Research Institute.
Şahin, Y., Akkaya, Y., & Taşdemir, M. A. (2021). Effects of freezing conditions on the frost resistance and microstructure of concrete. *Construction and Building Materials, 270*, 121458.
Shang, H., Cao, W.-Q., & Wang, B. (2014). Effect of fast freeze-thaw cycles on mechanical properties of ordinary-air-entrained concrete. *The Scientific World Journal, 2014*, 923032.
Takahashi, T., Itou, K., & Fuchigami, S. (2012). Development of pre-packed concrete trackbed for shinkansen. *Railway Technical Research Institute Report, 26*(2), 19–24.
Zhenshuang, W. (2011). Influence of fly ash on concrete permeability and frost resistance.

Publisher's Note